Inorganica Chimica Acta xxx (2014) xxx–xxx

Contents lists available at ScienceDirect

Inorganica Chimica Acta

journal homepage: www.elsevier.com/locate/ica

Rationalizing the formation and versatility of multinuclear metal complexes of bis(1-methyluracil-5-yl)methane as hybrids between classical calix[*n*]arenes and metallacalixaromatics

Anupam Khutia [a], Wei-Zheng Shen [a], Neeladri Das [a,1], Pablo J. Sanz Miguel [b,*], Bernhard Lippert [a,*]

[a] *Fakultät Chemie und Chemische Biologie, Technische Universität Dortmund, 44221 Dortmund, Germany*
[b] *Departamento de Química Inorgánica, Instituto de SíntesisQuímica y Catálisis Homogéna (ISQCH), Universidad de Zaragoza-CSIC, 50009 Zaragoza, Spain*

ARTICLE INFO

Article history:
Available online xxxx

Keywords:
Supramolecular chemistry
1-Methyluracil
Metallacalix[*n*]arenes
Platinum
Palladium

ABSTRACT

Metallacalix[*n*]arenes are a distinct class of metallacyclic compounds consisting of heteroaromatic rings L and square-planar *cis*-a_2M^{II} entities (M = Pt or Pd; a = NH_3 or amine; or a_2 = chelating diamine) instead of methylene bridges as in the classic calix[*n*]arenes. Here a series of hybrid compounds is described, which simultaneously have bridging $–CH_2–$ as well as *cis*-a_2M^{II} units, and uracil containing ligands L. Specifically, L = bis(1-methyluracil-5-yl)methane (**1**) and in one case a derivative of it, bis(1-methyluracil-5-yl)methylbenzene (**2**), have been reacted with *cis*-$[a_2M(H_2O)_2]^{2+}$ (with a = NH_3 or a_2 = 2,2′-bipyridine or bis(pyrazloyl-1-yl)propane) in water and products were isolated. Altogether X-ray crystal structures of eight metallacycles (complexes **3**–**6**, **8**–**11**) of M_2L_2, M_4L_2, and M_6L_6 stoichiometries have been determined as well as a second modification of **1**. In all closed metallacycles the 1-methyluracil entities are deprotonated with metals coordinating via N3 positions, and without exception the uracil rings adopt 1,3-alternate conformations. A special feature of ligand **1** in its twofold deprotonated form is its propensity to bind additional metal ions through its exocyclic oxygen functionalities. While O4 sites appear to be favored as secondary metal binding sites, linkage isomerism and involvement of O2 is likewise possible (compounds **4**, **9**, **10**). On the basis of the X-ray crystal structures, a reaction scheme is proposed which accounts for the different stoichiometries observed.

1. Introduction

In classical organic calix[*n*]arenes, *n* methylene groups bridge *n* para-substituted phenols, yielding cyclic compounds [1]. Depending on the rotational states of the phenol entities with respect to each other, calix[*n*]arenes can exist in a variety of conformers. Replacement of the CH_2 groups by numerous other groups or heteroatoms (e.g., O, NH, NR, S, SO_2, etc.) and of the phenols by other heterocyclic rings produces numerous types of “heterocalix[*n*]aromatics” [2]. Taking a further step in modification of organic calix[*n*]arenes, *cis*-L_2M^{II} entities with M = Pt or Pd and L being a variable donor ligand can likewise be utilized to substitute the bridging methylene groups, thereby generating metallacalix[*n*]arenes [3–6], a distinct subgroup of metallamacrocyclic compounds [7]. They display the characteristic *conformational flexibility* of their purely organic cousins, hence have the potential to occur as different conformers. Furthermore, they are to be differentiated from those metal complexes of calix[*n*]arenes, where metal coordination takes place through donor atoms within the rim and/or the bridging groups, or via dangling groups attached to the rims of the calix[*n*]arenes [8–10]. Applying substituted pyrimidines as heteroaromatic ligands, including the parent nucleobases uracil and cytosine, we and others have prepared and characterized a number of such compounds with *n* = 4 [3,4a–f], 6 [4f,5c], and 8 [5a], occasionally using also two different nucleobases and two different metal ions simultaneously. Our interest in metallacalix[*n*]arenes containing pyrimidine ligand not only relates to non-covalent interactions with DNA – some of these compounds display surprising effects on the structure of double-stranded DNA [11] – but also to host–guest chemistry with anions [4a,4f,12] and, surprisingly, even with cations [4c,13]. In fact, the propensity of these positively charged, hence cationic metallacycles to coordinatively bind additional metal ions via their exocyclic oxygen and/or deprotonated amino groups, is astonishing, although it reflects the behavior of numerous small metal complexes of heavy metal ions with pyrimidine

---

* Corresponding authors.
E-mail addresses: pablo.sanz@unizar.es (P.J. Sanz Miguel), bernhard.lippert@tu-dortmund.de (B. Lippert).

[1] Present address: Department of Chemistry, Indian Institute of Technology Patna, Patna 800013, Bihar, India.

http://dx.doi.org/10.1016/j.ica.2014.01.020

Please cite this article in press as: A. Khutia et al., Inorg. Chim. Acta (2014), http://dx.doi.org/10.1016/j.ica.2014.01.020

nucleobases as well as related amidate ligands [14]. As a result, multinuclear metal complexes are formed which frequently feature short intermetallic distances.

In an earlier communication [15], we have reported the design and synthesis of novel hybrids between classical calix[4]arene and metallacalix[4]arenes (Chart 1). The term "hybrid" has been coined since these metallacycles, based on uracil moieties, contained both methylene groups *and* square-planar *cis*-X_2Pt^{II} ($X = PPh_3$ or X_2 = 2,2′-bpy) units. They were synthesized by reacting the ditopic ligand bis(1-methyluracil-5-yl)methane $C_{11}H_{12}N_4O_4$ (**1**) with the corresponding *cis*-X_2Pt^{II} entities. In continuation of our efforts to exploit the coordination properties of **1**, we herewith report the synthesis and characterization (^1H NMR and single crystal X-ray crystallography) of several representative examples of this new class of hybrid metallacycles. A derivative of **1** (bis(1-methyluracil-5-yl)methylbenzene, ligand **2**) is also being dealt with in this article. **2** extends the list of related polytopic ligands containing 1-methyluracil-5-yl entities recently reported by us [16].

At an early stage of our studies it became evident that **1** gives rise to products of different stoichiometries and nuclearities, in part depending on the nature and steric requirements of the co-ligands L of the square-planar Pt^{II} ion. By further varying these co-ligands ($L = NH_3$; L_2 = bis(pyrazol-1-yl)propane, bipzp) and also by substituting in part Pt by Pd, the attempt was made to generate a unifying reaction scheme which explains the different stoichiometries and nuclearities without explicitly differentiating between the heterocyclic ligand (**1** or **2**), the metal entities (Pt^{II} or Pd^{II}), and the co-ligands L_2.

2. Results and discussion

2.1. Second polymorph of bis(1-methyluracil-5-yl)methane (1a)

Reaction of 1-methyluracil (1-MeUH) with paraformaldehyde under HCl-acidic conditions and recrystallization of the crude product from H_2O/EtOH yields a monohydrate of **1**, which crystallizes in the triclinic crystal system and space group $P\bar{1}$ [15,17]. We have now isolated **1** as a second polymorph **1a** (monoclinic, space group $P2_1/c$; monohydrate) during an unsuccessful attempt to synthesize a silver complex by reacting $AgNO_3$ with **1** in a 1:1-mixture of H_2O and MeOH. The colorless crystals recovered after cooling the solution proved to be **1a**. The two modifications **1** and **1a** differ essentially in the mutual disposition of the uracil entities, which is transoid in the case of **1a**, forming a dihedral angle of 83.51(3)°. In **1**, both uracil rings were tilted 77.82(9)° in an intermediate disposition between cisoid and transoid, namely, with the C6 site of one uracil pointing roughly toward the centroid of the other (Fig. 1). Supramolecular arrangement of **1a** is dominated by ribbons in a zig–zag fashion, which are assembled by twofold hydrogen bonded (N3a···O2b′, 2.8421(16) Å; O2a···N3b′, 2.8045(16) Å) units of the molecule along the *c* axis. Water molecules of crystallization (O1w) join parallel ribbons (O1w···O4a, 2.8109(17) Å; O1w···O4b′, 2.9144(17) Å), thus forming a 3D polymeric network.

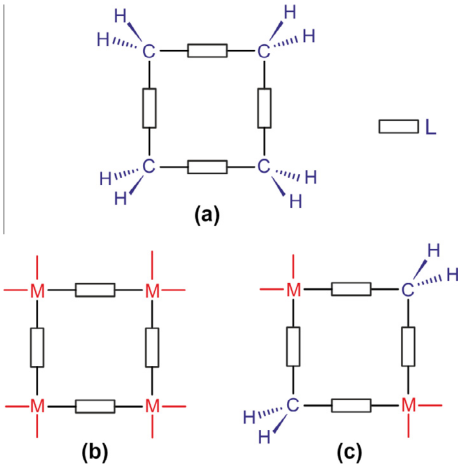

Chart 1. Schematic views of (a) classical calix[4]arene, (b) metallacalix[4]arene, and (c) hybrid between (a) and (b).

2.2. Synthesis of bis(1-methyluracil-5-yl)methyl-benzene (2) and comparison of its pK_a value with those of 1

The ligand bis(1-methyluracil-5-yl)methyl-benzene (**2**) was synthesized by the acid-catalyzed condensation of benzaldehyde with 1-methyluracil (1-MeUH) (Scheme 1). The product was obtained as a white solid in 94% yield. The ^1H NMR spectrum of **2** (recorded in Me_2SO-d_6) is consistent with its composition (Supporting Information). The connectivity between the two 1-MeUH units and the benzylic carbon is clearly indicated by the presence of a 1H singlet at δ 5.09 and a 2H singlet δ 7.03 due to the hydrogen at benzylic position and the hydrogen attached to C6 of each uracil unit, respectively. The pK_a values of **2** were determined by use of pD dependent ^1H NMR spectroscopy. A single pK_a of 10.05 ± 0.04 (converted from D_2O to H_2O; average of H6 and N1–CH_3 resonances) was obtained for two overlapping deprotonation steps, virtually identical with that for **1** (10.02 ± 0.02) [15]. Individual pK_a values of **2** are therefore in the range of ca. 9.75 to ca. 10.35 (Supporting Information). As compared to 1-methyluracil (pK_a = 9.63 ± 0.05) [18], the 1-methyluracil-5-yl entities in **2**, like in **1**, are thus somewhat less acidic than the parent ligand 1-MeUH itself. This is reminiscent of the situation with 1-methylthymine, which likewise has a lower acidity (pK_a = 10.3) [19] than 1-methyluracil, as it carries a methyl group at the C5 position. Unlike with **1** (**1a**), attempts to obtain X-ray-quality single crystals of **2**, failed.

2.3. Synthesis and characterization of $[Pd(bipzp)(1')]_2 \cdot 13H_2O$ (3)

Reaction of $[Pd(bipzp)(H_2O)_2](NO_3)_2$ (bipzp = bis(pyrazol-1-yl)propane), obtained *in situ* by treatment of $PdCl_2$(bipzp) [20] with $AgNO_3$, and **1** in a 1:1 ratio in water, pH 9.0, yielded the neutral metallacalixarene $[Pd(bipzp)(\mathbf{1'})]_2 \cdot 13H_2O$ (**3**) (with **1′** = dianion of **1**, deprotonated at the two N3 positions of the uracil rings) (Scheme 2). The ^1H NMR spectrum of **3** indicated the formation of a single and finite macrocyclic species, as evident from the presence of sharp peaks corresponding to Pd^{II}(bipzp) and **1′**. Resonances of the three protons H3′, H4′, and H5′ of bis(pyrazol-1-yl)propane are observed at 8.12 (d), 6.45 (t) and 7.63 (d) ppm, respectively, and of the CH_3 protons of bipzp as a singlet at

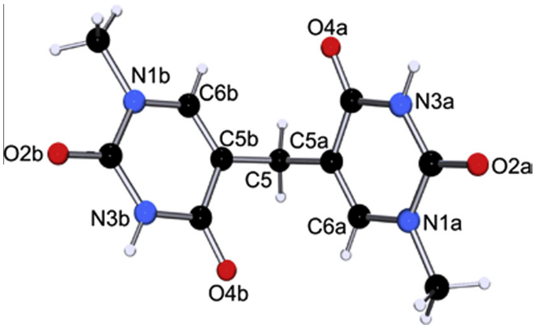

Fig. 1. View and atom numbering of bis(1-methyluracil-5-yl)methane (**1a**) (monohydrate, second polymorph).

Please cite this article in press as: A. Khutia et al., Inorg. Chim. Acta (2014), http://dx.doi.org/10.1016/j.ica.2014.01.020

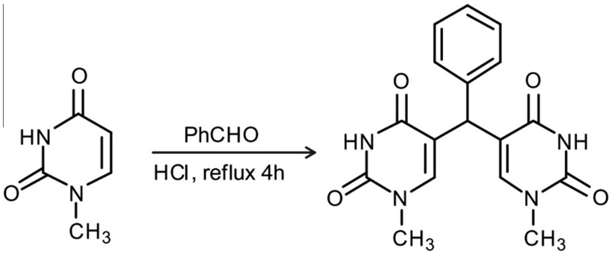

Scheme 1. Formation of ligand **2**.

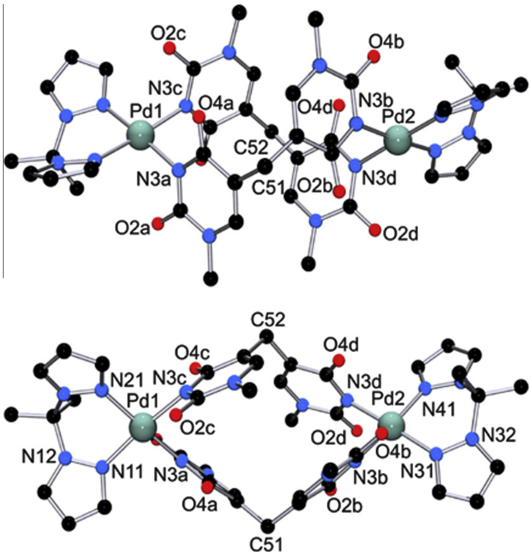

Fig. 2. Two views and atom numbering scheme of neutral complex **3**.

2.99 ppm. The singlet at 7.14 ppm corresponds to C6H of the uracil units in **1′**.

The structure of **3** was determined by X-ray crystallography. Light yellow, prism shaped X-ray quality single crystals were obtained upon slow evaporation of an aqueous solution of the complex. A view of compound **3** is shown in Fig. 2. It reveals that **3** is a metallacalixarene in which two Pd^{II}(bipzp) units are bridged by two dianions of **1**, hence **1′**, via the N3 deprotonated sites in a cyclic fashion. Both bridging ligands **1′** are transoid as far as the two uracil rings are concerned, and the pairs of coordinating uracil entities are mutually *head–tail* at each metal center. Hence the four uracils adopt a *1,3-alternate* conformation according to the metallacalix[4]arene nomenclature. The cation, which represents a chiral double helicate and its mirror image are present in a 1:1 mixture in the crystal, as required by space group $P\bar{1}$. The overall shape of this Pd$_2$ metallacycle **3** is thus similar to the Pt$_2$ compound that we have reported in our previous communication [15], although less regular than the former. The Pt$_2$ and Pd$_2$ metallacycles differ from similar bis(pyridine-4-yl)methane [21] and bis(pyridine-4-yl)dimethylsilane [22] metallacycles in that the latter are achiral and do not provide the potential of calixarenes to adopt different rotamer states of its heterocyclic pyridine components. The four atoms comprised of two Pd atoms and two C atoms of the methylene bridges in **3** are located nearly in a plane, producing a rhomboid shape. Intermolecular dimensions are 8.9436(4) Å (Pd···Pd) and 6.424(3) Å (CH$_2$···CH$_2$). The tilt angles between the uracil rings and this plane are 81.4(6)°, 80.86(5)°, 72.04(5)°, and 69.71(5)°, for rings a, b, c, and d, respectively. Considering these angles, it can be concluded that **3** exists in a *pinched 1,3-alternate* conformation. The average distances between two alternate uracil rings range from 4.36 Å at the lower rim to 5.72 Å at the upper rim. The average distance between the centroid of two alternate uracil rings is 5.01 Å. Other structural features of **3** are as follows: The geometry around each Pd is close to square-planar, with a N11–Pd1–N21 angle of 89.22(8)°, a N3a–Pd1–N3c angle of 87.58(8)°, and a N21–Pd1–N3a angle of 175.03(9)°. The distance between O4 sites of opposite uracil rings are 6.334(3) Å (ring a–d), and 6.473(3) Å (ring b–c) (wide rim), while the N1-methyl groups of opposite uracil rings are 3.821(4) Å (ring a–d) and 3.666(4) Å (ring b–c) apart (narrow rim). The “height” of the calixarene, as defined in this case by the average distances between N-methyl groups, is ca. 9.0 Å.

The most outstanding aspect of the crystal packing of **3** is the water cluster assembled therein. It is rarely seen a crystal structure of about 150 atoms including two Pd^{II} ions and 13 fully occupied and crystallographically different water molecules with such a quality of the data. Furthermore, we could find an adequate orientation of the hydrogen atoms within the H-bonding pattern. The nature of this water cluster is two-dimensional and extends along the *a* axis. Dimensions are comparable to those of a water cluster nanotube [23]. However, the water molecules of **3** are disposed following a central backbone of fused squares and hexagons (Fig. 3). Some additional hexagons and pentagons are also present in the skeleton. Concretely, the central hexagon “H1” {O1w–O4w–O12w–O7w–O11w–O5w} shares their alternate edges with three different squares “S1” {O4w–O12w–O3w–O10w}, “S2” {O7w–O11w–O7w′–O11w′}, and “S3” {O1w–O5w–O1w′–O5w′}. An additional hexagon “H2” {O6w–O2w–O9w–O7w–O11w–O5w} results from the fusion of “H1”, “S2”, and the pentagon “P1” {O1w–O5w–O11w–O13w–O8w}, which is also merged with “H1” and

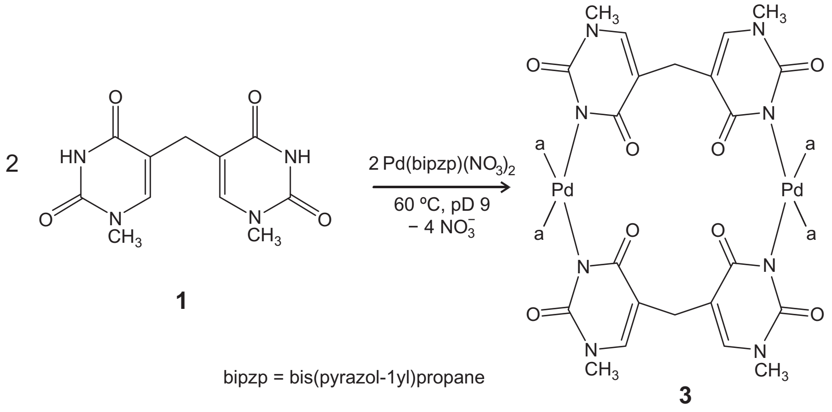

Scheme 2. Synthesis of Pd$_2$ complex **3**. Deprotonation of **1** is achieved by means of NaOH.

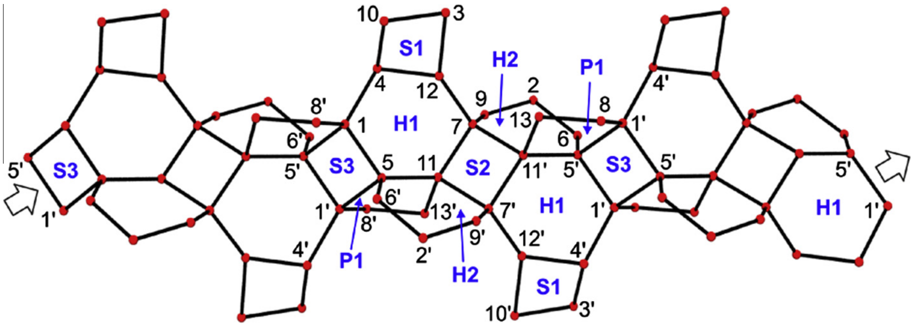

Fig. 3. Packing of the water cluster present in **3**.

“S3”. Hydrogen bonding distances of closed water cluster are listed in Table 1. Growing of the two dimensional water cluster follows a 120° zig-zag degree along the {H1 → S2 → H1 → S3 → }$_n$ direction. Analogously, the definition of an alternative growing along the {S3 → P1 → H2 → S2 → H2 → P1 → }$_n$ direction would be also valid. This intriguing water organization is anchored to complex **3** via the carbonyl O2 and O4 groups: O2a···O8w, 2.796(3) Å; O4a···O9w, 2.736(3) Å; O2b···O3w, 2.658(2) Å; O4b···O6w, 2.748(3) Å; O2c···O2w, 2.701(3) Å; O4c···O10w, 2.841(2) Å; O2d···O2w, 2.716(3) Å; O4d···O3w, 2.869(3) Å.

From model building it appears perfectly reasonable to assume that a cone conformer of **3** is likewise feasible, in which the two bis(1-methyluracilate-5-yl)methane ligands are oriented cisoid. In this case O2 sites are pairwise adjacent at close distances, as are O4 sites. Either proton binding, hence the presence of a mono-anionic species of **1**, metal crosslinking through pairs of adjacent oxygen atoms, or the presence of a templating agent favoring a cone conformer structure, would appear helpful in stabilizing such a structure.

2.4. Synthesis and characterization of $[\{Pd(bipzp)(1'\text{-}N3)\}_2(Ag\text{-}O2,O4)]_n(NO_3)_n\cdot 15H_2O$ (**4**)

It has been previously reported by us that the cyclic cation $[Pt(en)(UH\text{-}N1,N3)]_4^{4+}$ is markedly stabilized in the *1,3-alternate* conformation (in solid state) due to the formation of intramolecular hydrogen bonds between exocyclic hydroxyl and exocyclic carbonyl groups of the rare uracil anion (UH) tautomer [3]. In solution and following deprotonation of the UH monoanion to the U dianion at basic pH, the cation exists in an equilibrium mixture of *cone* and *1,3-alternate* conformations. Furthermore, it has been demonstrated that Ag$^+$ ions can spontaneously deprotonate UH ligands and are able to convert the *1,3-alternate* conformer to the cone conformer in acidic medium, thereby producing the octanuclear species $[Pt(en)(UH\text{-}N1,N3,O2)Ag]_4^{8+}$ [13a]. As has been mentioned previously, the oxo-surface formed by the exocyclic atoms of uracil nucleobases provides a platform for binding four Ag$^+$ ions. The four uracil moieties in metallacalixarene **3** provide altogether eight uncoordinated exocyclic oxygen atoms which could act as anchor sites for additional metal ions. In order to test its likelihood, an aqueous solution of **3** was mixed with silver nitrate, anticipating a similar coordination behavior as with $[Pt(en)(UH\text{-}N1,N3)]_4^{4+}$. However, the product obtained proved to be a coordination polymer rather than a discrete multinuclear entity, in which the two **1**′ ligands retain their transoid orientations as well as the *head–tail* arrangement with respect to the two Pd centers, and hence the *1,*

Table 1
Hydrogen bonding distances [Å] including hydrogen atoms involved in the water cluster of **3**.

3			
O1w(H1w)···O5w	2.786(2)	O7w(H14w)···O9w	2.713(2)
O1w(H2w)···O5w[a]	2.823(3)	O8w(H15w)···O2a[e]	2.796(3)
O2w(H3w)···O2c[b]	2.701(3)	O8w(H16w)···O1w	2.903(3)
O2w(H4w)···O2d	2.716(3)	O9w(H17w)···O2w	2.808(3)
O3w(H5w)···O4d[c]	2.869(3)	O9w(H18w)···O4a[b]	2.736(3)
O3w(H6w)···O2b[c]	2.658(2)	O10w(H19w)···O4c[e]	2.841(3)
O4w(H7w)···O1w	2.852(3)	O10w(H20w)···O3w[f]	2.776(3)
O4w(H8w)···O10w	2.790(3)	O11w(H21w)···O7w[g]	2.784(3)
O5w(H9w)···O6w	2.748(2)	O11w(H22w)···O7w[a]	2.793(3)
O5w(H10w)···O11w[a]	2.804(3)	O12w(H23w)···O7w[f]	2.877(3)
O6w(H11w)···O2w	2.806(3)	O12w(H24w)···O4w	2.801(3)
O6w(H12w)···O4b	2.748(3)	O13w(H25w)···O8w[e]	2.771(3)
O7w(H13w)···O12w[d]	2.717(3)	O13w(H26w)···O11w[e]	2.825(3)

Symmetry codes: [*a*] $-x+1, -y, -z+1$; [*b*] $x-1, y, z$; [*c*] $-x+1, -y+1, -z$; [*d*] $-x, -y, -z+1$; [*e*] $-x+1, -y+1, -z+1$; [*f*] $-x, -y+1, -z+1$; [*g*] $x+1, y, z$.

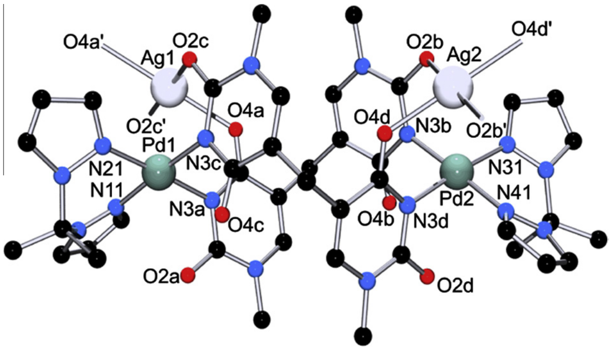

Fig. 4. Section of polymeric structure of $[\{Pd(bipzp)(\mathbf{1}'\text{-}N3)\}_2(Ag\text{–}O2,O4)]_n(NO_3)_n\cdot 15H_2O$ (**4**).

Table 2
Hydrogen bonding distances [Å] within the crystal packing of **4**.

4			
O1w···O4b	2.784(15)	O5w···O4c	2.813(18)
O1w···O2w[a]	2.780(17)	O6w···O9w	2.78(2)
O1w···O8w	2.778(17)	O6w···O13w	2.56(3)
O1w···O11w	2.67(3)	O7w···O2b[e]	2.83(2)
O2w···O5w[b]	2.727(19)	O7w···O11	2.31(3)
O3w···O2d[b]	2.839(15)	O7w···O14w	2.63(3)
O3w···O4w[a]	2.711(17)	O9w···O9w[a]	2.81(4)
O3w···O5w[a]	2.83(2)	O9w···O11w	2.84(3)
O3w···O8w[c]	2.74(2)	O10w···O11w	2.85(3)
O4w···O2a	2.754(18)	O10w···O12w	2.92(4)
O4w···O15w[d]	2.87(3)	O12w···O11	2.83(4)
O5w···O2a	3.053(14)	O12w···O13	3.61(5)

Symmetry codes: [*a*] $1-x, 1-y, -z$; [*b*] $x, y-1, z$; [*c*] $-x, 1-y, -z$; [*d*] $2-x, 1-y, -z$; [*e*] $-x, 1-y, 1-z$.

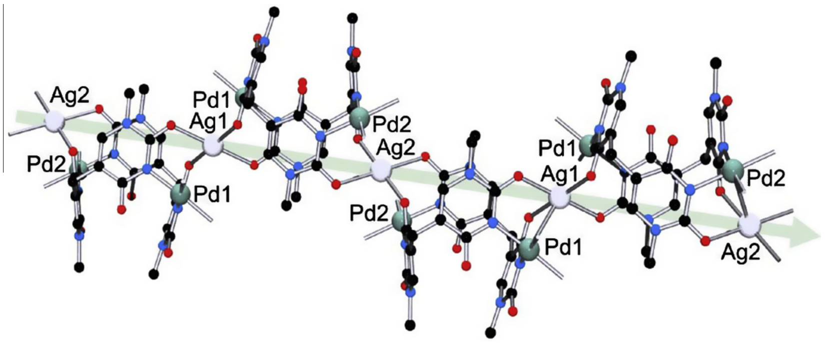

Fig. 5. Schematic view of the extended structure of **4** along the [1 1 0] direction (green arrow) displaying the alignment of the silver atoms. Hydrogen atoms and bipzp ligands attached to the Pd^{II} ions are omitted for clarity. (For interpretation of the references to color in this figure legend, the reader is referred to the web version of this article.)

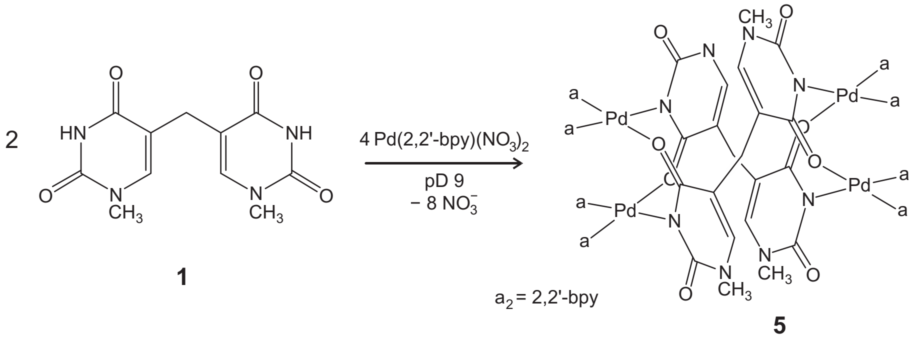

Scheme 3. Synthesis of Pd_4 complexes **5**.

3-alternate arrangement of the four uracil residues. According to the results of the crystallographic analysis of **4**, silver ions bridge adjacent metallacalixarene units, thereby generating the mixed-metal complex **[{**Pd(bipzp)(**1**′-*N3*)}$_2$(Ag–*O2,O4*}]$_n$·15H_2O. A segment of the coordination polymer **4** is depicted in Fig. 4. Each Ag^+ ion is coordinated by four exocyclic oxygen atoms of the uracilato ligands, via two O2 and two O4 atoms. This mixed O2,O4 coordination by two uracilate ligands, although seen before [24], appears to be less common than a sequential coordination of O4 sites first, and O2 sites only second.

The geometry around the silver ion is square-planar, which is the least common geometry as far as coordination chemistry of Ag(I) is concerned [25], even though it has some precedence in a Pt,Ag,1-MeU complex [26]. There is distortion within the square-planar coordination geometry of the Ag^+ ion in that two *trans*-Ag–O bonds are longer than the other two: The Ag1–O2c bond (2.380(10) Å) is longer than the *cis*-Ag1–O4a bond (2.307(8) Å). Similarly, the Ag2–O2b bond (2.463(8) Å) is longer than the *cis*-Ag2–O4d bond (2.247(10) Å). The average Ag–O bond length of 2.35 Å suggests relatively strong coordination bonds. Crystallographically, Ag^+ ions are sitting on a center of inversion as the coordinating ligands are the same. For each Ag^+ ion, two Pd^{II} moieties are residing in axial positions, with intermetallic distances of 2.9655(11) Å (Pd1–Ag1) and 3.0503(10) Å (Pd2–Ag2). Surprisingly these distances are longer than those in mixed Pt, Ag complexes with tetrahedral Ag geometries and 1-MeU ligands [27] and thus suggest at most very weak Pd–Ag interactions in **4** as well as negligible tetragonal distortion about the square planar environment of both Ag and Pd centers. Clearly, these intermetallic distances are significantly longer than those observed in heteronuclear Pt, Ag complexes with dative Pt → Ag bonds [28]. As far as the structural details of the individual Pd_2-macrocycle **4** are concerned, there are only minimal deviations from **3**.

Silver atoms within the 1D coordination polymer are aligned along the [1 1 0] direction, displaying intermetallic distances of 8.9969(9) Å (Ag1–Ag2). As in the case of compound **3**, the crystal packing retains a high amount of crystallized water, namely 15 water molecules per cation of **4**. They form an intriguing two dimensional hydrogen bonding pattern connecting the cations of **4** and the nitrate anions. Hydrogen bond distances are listed in Table 2 (Fig. 5).

2.5. Synthesis and characterization of ht,ht-{[Pd(2,2′-bpy)]$_2$(1′)}$_2$(H_3O)(NO_3)$_5$·8H_2O (**5**)

Reaction of [Pd(2,2′-bpy)(H_2O)$_2$](NO_3)$_2$ in water with **1** in 1:1-ratio yielded a Pd_4 “open molecular box” *ht,ht*-{[Pd(2,2′-bpy)]$_2$(**1**′)}$_2$(H_3O)(NO_3)$_5$·8H_2O (**5**) (Scheme 3). **5** was characterized by ^1H NMR spectroscopy, elemental analysis, and eventually X-ray crystallography. The formation of a single and finite macrocyclic species was indicated by the ^1H NMR spectrum of **5** due to the presence of sharp peaks corresponding to Pd^{II}(2,2′-bpy) and **1**′. Relative intensities of the resonances of **1**′ and 2,2′-bpy are consistent with the above composition. The chemical shifts in D_2O (δ, 7.60, 7.23) of the two different H5 resonances of the 2,2′-bpy ligand (present in a 1:1 ratio, Supporting Information) clearly prove a *head–tail* orientation within two stacked Pd^{II}(2,2′-bpy) entities [29].

This conclusion was confirmed by the results of the X-ray crystal structure determination of **5**. A view of the cation of **5** is depicted in Fig. 6. It is closely isostructural to the corresponding Pt complex reported earlier by us [15] and its other modification (**6**, see below). Each Pd is simultaneously bonded to a deprotonated N3 position of **1** and to an O4 site, hence the **1**′ ligands in each dinuclear Pd_2 unit are *head–tail*. As observed for the other complexes (**3** and **4**), uracil moieties retain their transoid orientations

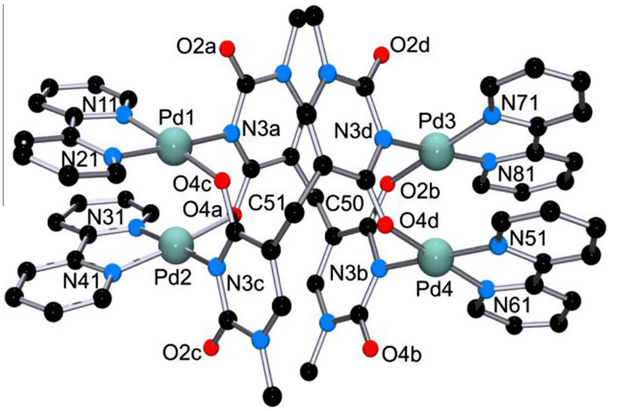

Fig. 6. View of the crystal structure of cation **5**.Water molecules of crystallization have been omitted for clarity.

of the N1–CH_3 groups and the overall 1,3-alternate conformation of the uracil rings. The cation thus represents a chiral double helicate with two dipalladium stacks instead of two single metal ions, as in **3**. Unlike **3** with its rhomboid shape, cation **5** looks more like an open box with comparable distances between the CH_2 groups (7.00(4) Å) and the Pd ions across the square (Pd1–Pd3, 7.293(3) Å; Pd2–Pd4, 7.186(3) Å. As compared to **3**, the “height” of metallacalixarene **5** (distances between N-methyl groups) is higher by ca. 0.4 Å. The distance between two Pd centers within the stacked Pd(2,2′-bpy) entities are 2.863(3) Å (Pd1–Pd2) and 2.844(3) Å (Pd3–Pd4), comparable to other stacked Pd(2,2′-bpy) entities [5b]. The 2,2′-bpy planes are rotated slightly, by 6.8° (average).

The crystal packing of **5** is dominated by π–π stacking interactions between the 2,2′-bpy rings of the cations (Pd1,Pd2 rings, 3.5 Å), which form infinite arrays. Combination of further π–π stacking involving the (Pd3,Pd4)-2,2′-bpy rings builds a two-dimensional stacking network which extends along the *bc* plane. An additional feature of the crystal packing is the formation of a hexagonal water cluster, to which the nitrate ligands and HNO_3 are hydrogen bonded (Supporting Information): O1w···O4w, 2.48(4) Å; O4w···O3w, 2.65(4) Å; O3w···O6w, 2.69(4) Å; O6w···O2w, 2.83(4) Å; O2w···O5w, 2.72(3) Å; O5w···O1w, 2.73(4) Å; O1w···O11, 2.86(4) Å; O4w···O53, 2.50(4) Å; O3w···O33, 2.73(5) Å; O6w···O13, 2.84(5) Å; O6w···O43, 2.73(4) Å; O2w···O22, 2.74(4) Å; O5w···O2b, 2.74(4) Å. Concerning the location of the HNO_3 proton, we could deduce, from the short O1w–O4w and O4w–O53 distances the existence of a $H_5O_2^+NO_3^-$ unit which in principle could stabilize this proton.

2.6. Second polymorph of ht,ht-{[Pt(2,2′-bpy)]$_2$(1′)}$_2$(NO_3)$_4$·12H_2O (**6**)

The reaction of [Pt(2,2′-bpy)(H_2O)$_2$](NO_3)$_2$ with **1** in a 2:1-ratio yielded a second polymorph of the Pt_4 “open molecular box” {[(2,2′-bpy)Pt]$_2$(**1′**)}$_2$(NO_3)$_4$·12H_2O (**6**), which has been previously been reported by us (compound **3** in Ref. [15]). The cation is depicted in the Supporting Information, with some selected bond distances and angles given. There are no major differences in bond lengths and bond angles as compared to the reported structure. In the crystal lattice of **6**, cations align in infinite piles of π–π stacked 2,2′-bpy ligands.

The ^1H NMR resonances of **6** (Supporting Information) have been previously assigned [15]. A comparison with the ^1H NMR spectrum of **5** (Supporting Information) reveals virtual identical shifts of 7.93 ppm for the uracil H6 signals in the two complexes, but some differences in bpy resonances, and in particular of one of the two non-equivalent bpy-H6 doublets (8.35 ppm in **6**; 7.79 ppm in **5**; second sets buried under signals between 8.0 and 8.2 ppm). Differences in overlap of the stacked bpy rings may account for it.

2.7. h,t-{[(2,2′-bpy)Pt]$_2$[1-MeU-N3,O4-CH(Ph)-1-MeUH]$_2$}$^{2+}$ (**7**)

Reaction of [Pt(2,2′-bpy)(H_2O)$_2$](NO_3)$_2$ with **2** in water yielded the dinuclear metal complex **7** (Scheme 4), which was identified by a preliminary X-ray analysis.[2] It establishes a *head–tail* orientation of the two coordinating uracil entities. We mention its existence in the context of discussions regarding possible primary products during reactions of *cis*-a_2M^{II} with bis(uracil-5-yl) type ligands (see Section 2.9).

2.8. cis-Diammineplatinum(II) complexes of **1**: multiple products

Reactions carried out between *cis*-$(NH_3)_2Pt^{II}$ and **1** on a ^1H NMR scale in D_2O indicated the formation of multiple products side by side, depending somewhat on reaction conditions (pH, concentration, ratio between metal and **1**). A typical example is given in the Supporting Information. It reveals (at least) nine uracil-H6 singlets, none of which is due to free **1**. Five of these singlets correspond to complexes described below; the remaining four resonances are presently unassigned. Altogether four distinct compounds (**8–11**) were crystallized and X-ray structurally characterized, as outlined below. Although it proved difficult to selectively isolate all four of the complexes in good yields, we report on our findings as these provide insight into the complexity of metallacalix[*n*]arene systems containing pyrimidine nucleobases, and allow for justified speculations regarding the existence of additional species.

2.8.1. ht,ht-{[cis-Pt(NH_3)$_2$]$_2$(1′)}$_2$(NO_3)$_4$·11H_2O (**8**)

Complex **8** is a structural analogue of the tetranuclear complexes **5** and **6**. The cation consists of four *cis*-$(NH_3)_2Pt^{II}$ units coordinated to two **1′** ligands, in which **1′** adopts a transoid structure, with the Pt ions bonded pairwise to N3 and O4 sites of the uracil rings and mutually arranged in *head–tail* fashion. The cation is chiral as a consequence of the *head–tail* arrangement of the uracilate rings. Both enantiomers are present in the lattice of **8**. Fig. 7 gives a view of the cation of **8**.

Salient structural features of **8** are as follows: The uracil rings in each ligand **1′** are almost perpendicular to each other, with dihedral angles of 89.0(6)° and 87.5(6)°. As compared to **5** and **6**, cation **8** is more extended as far as intramolecular distances between the methyl groups of **1′** (C1a–C1c, 10.33(3) Å; C1b–C1d, 10.29(4) Å) and the methylene bridges (C51–C52, 6.70(2) Å) are concerned. Distances between the Pt centers across the calix core are 7.2450(11) Å (Pt1–Pt4) and 7.3261(11) Å (Pt2–Pt3), hence longer than in the cases of **5** and **6**. On the other hand, Pt–Pt distances within the dimetal cores are also significantly longer 2.9667(12) Å (Pt1–Pt2) and 2.9659(13) Å (Pt3–Pt4) in **8**, probably a consequence of the replacement of the well-stacking 2,2′-bpy ligands by ammonia ligands. This difference in metal–metal contacts is accompanied by slightly larger torsional angles of adjacent Pt coordination planes in **8** (7.5(6)° and 8.7(8)°). Additional bond distances and angles are provided in the Supporting Information. As in the previous cases, a complicated hydrogen bonding pattern assembled by the cation of **8**, counter anions and numerous water

---

[2] Although of poor quality, and therefore not shown here, X-ray analysis of **7** is consistent with a *head–tail* structure of the cation (Pt–Pt, 2.8597(4) Å) and a cisoid orientation of the coordinated uracilate and the terminal uncomplexed uracil (dihedral angle 84.78(14)°). The stereogenic centers at the two phenyl bonded C atoms are *R* and *S* configurated, hence the cation represents a *meso* form.

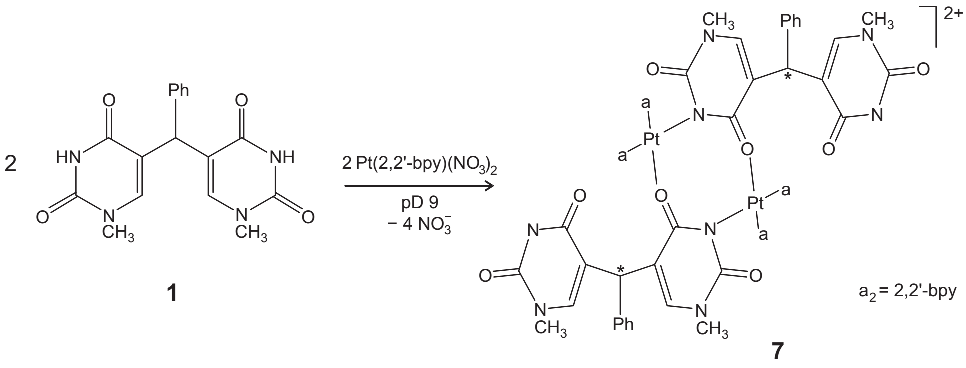

Scheme 4. Formation of complex **7**.

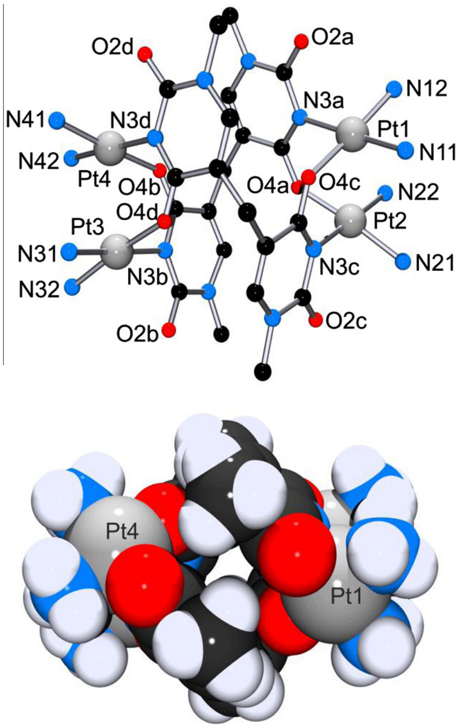

Fig. 7. Side view (top) and space filling representation (bottom) of cation of **8**.

molecules of crystallization (11 in this case) is present in the crystal packing.

As expected, the ^{1}H NMR spectrum of **8** is very simple. In D_2O only three singlet resonances in the proper relative intensities are observed, at 7.45 ppm (H6), 3.54 ppm ($N1–CH_3$), and 3.08 ppm (CH_2).

2.8.2. hh,ht-{[cis-Pt(NH_3)$_2$]$_2$(1′)}$_2$(NO_3)$_4$·9.5H_2O (**9**)

In the course of our studies, also a crystalline product was isolated whose ^{1}H NMR spectrum revealed the presence of four sets of 1-MeU resonances in a 1:1:1:1- ratio (Fig. 8).

X-ray crystallography (Fig. 9) subsequently proved the origin of this spectral feature by revealing that the two ligands **1**′ displayed different coordination modes: While one of the two bridging ligands in **9** exhibits the metal binding patterns seen in **5**, **6**, and **8**, the second ligand uses N3 and O4 as coordination sites on one edge, and N3 and O2 at the other edge. As the transoid orientations of the two uracil rings are maintained in both cases, a simple slippage movement has occurred at one of the two edges (Scheme 5).

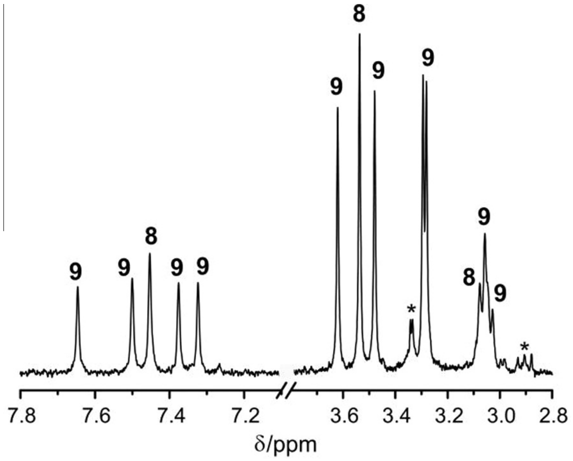

Fig. 8. Sections of ^{1}H NMR spectrum (D_2O) of compound **9** with an admixture of **8** and an unknown impurity (*). Four sets of uracil-H6 and -CH_3 signals are observed.

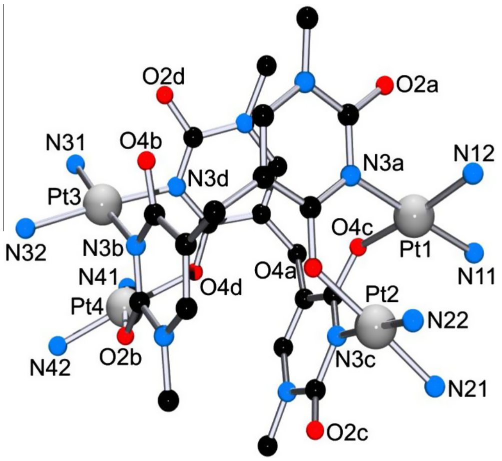

Fig. 9. View of molecular cation **9**.

From model building it is evident that this slippage causes relatively minor structural changes as compared to **8**. The main difference is that at the site of slippage, one Pt is now coordinated to two N3 sites, while the other Pt is bonded to O4 and O2 sites of two different uracil rings. We call this bonding situation, somewhat simplified, *head–head*, although we are aware that in the strict sense this term should be reserved for situations in which one metal is coordinated to two N3 sites, whereas the other one is coordinated to *identical* sites, hence *either* two O4 *or* two O2 donor atoms.

Please cite this article in press as: A. Khutia et al., Inorg. Chim. Acta (2014), http://dx.doi.org/10.1016/j.ica.2014.01.020

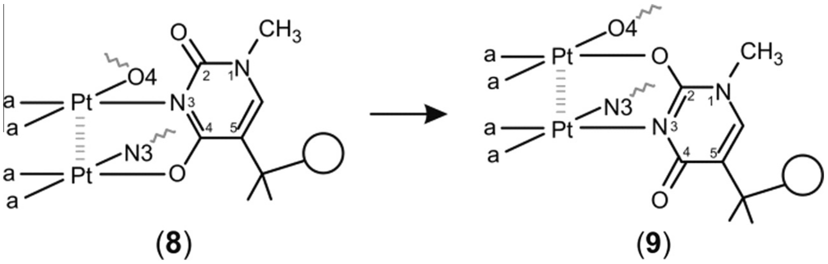

Scheme 5. Structural relationship between Pt_2 edge in **8** and **9**: Slippage of uracil ring from N3,O4 bridge to O2,N3 bridge.

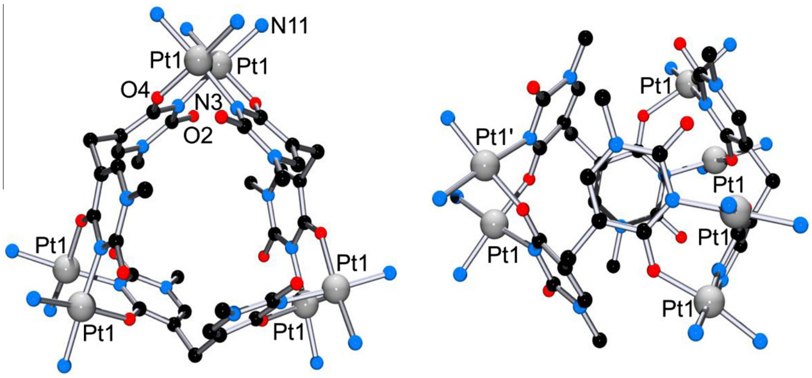

Fig. 10. Top and side views of the highly symmetrical cation **11**.

Structural details of **9** are as follows: The unit cell contains two crystallographically different cations of **9**, which present an almost identical geometry. The high number of water molecules of crystallization – 21 crystallographically different occupied sites in this case – impedes a good quality of the collected data. Tilt angles values between the uracil rings in each ligand **1**′ are slightly distant from perpendicularity in comparison with **5**, **6**, and **8** (88.1(4)°, 83.8 (5)°, 84.9(4)°, 80.0(6)°). Due to the coordination slippage, the cations of **9** display marked differences between C1–C1 distances: 8.52(3) Å (C1d–C1e) and 8.56(3) Å (C1e–C1g) in the short edge, and 10.59(3) Å (C1a–C1c) and 10.62(3) Å (C1f–C1h) in the long edge. Distances between adjacent platinum atoms are similar to the found in the previous cases (Pt1–Pt2, 2.9152(11) Å; Pt3–Pt4, 2.9242(12) Å). Distances between the platinum ions, and distances between the CH_2 bridges across the calix cores are in this case significantly longer, also a consequence of the different geometry: Pt1–Pt3, 7.9569(11) Å; Pt2–Pt4, 7.7411(11) Å; Pt5–Pt7, 8.0097(12) Å; Pt6–Pt8, 7.9327(11) Å; C51–C52, 6.82(2) Å; C53–C54, 6.75(2) Å. The crystal packing presents a high density of hydrogen bonding between cations, nitrate anions and water molecules.

Slippage could occur, in principle, also at the other edge of the metallacycle. The mixed Pd,Ag complex **4** provides an excellent example to support this option, in that substitution of the Ag^+ ions by square-planar *cis*-a_2M ($M = Pt^{II}$ or Pd^{II}) entities would generate exactly such a product with twofold N3 binding of two of the metals, and mixed O2,O4 binding of the two others, hence *head–head* orientations at both edges of the metallacycle (in the restricted definition, see above). In the ^1H NMR, this coordination scheme would result again in a simplification, namely to a single set of resonances of **1**′.

2.8.3. A 2:1-adduct of **8** and **9**: Compound **10**

The X-ray analysis of yet another species isolated from a reaction mixture of *cis*-$(NH_3)_2Pt^{II}$ and **1** upon slow evaporation proved to be a 2:1-adduct of compounds **8** and **9**, namely 2[*ht,ht*-{[*cis*-$Pt(NH_3)_2]_2$(**1**′)}$_2$]·[*hh,ht*-{[*cis*-$Pt(NH_3)_2]_2$(**1**′)}$_2$]$(NO_3)_{12}\cdot 16H_2O$ (**10**). The two different cations in **10** do not differ much with regard to structural details from their individual components, as observed in a preliminary X-ray structure (Supporting Information).

2.8.4. Hexanuclear complex *ht,ht,ht*-{[*cis*-$Pt(NH_3)_2$(1′)]$_3$$(NO_3)_6\cdot 9H_2O$ (**11**)

As a final product isolated from reaction mixtures of *cis*-$(NH_3)_2$ Pt^{II} and bis(1-methyluracil-5-yl)methane (**1**) we wish to report on a cyclic complex comprised of three Pt_2 stacks and three dianions of **1**. *ht,ht,ht*-{[*cis*-$Pt(NH_3)_2$(**1**′)]$_3$$(NO_3)_6\cdot 9H_2O$ (**11**) forms in the presence of an excess of Pt over **1** (2:1) at pH 5. Needle-shaped, light green crystals of **11** were isolated from a reaction mixture that had turned dark blue, presumably due to partial oxidation of Pt, similar to the situation with "platinum pyrimidine blues" [30]. The concentration of the solution from which **11** was obtained, was five times higher than that from which the tetranuclear complexes **8**, **9**, and **10** were isolated. Fig. 10 provides two views of the hexanuclear cation **11**. As can be seen, all three ligands **1**′ are transoid and all three Pt_2 pairs are coordinated in *head–tail* fashion through N3 and O4 sites of the anionic uracil rings. While the top view of **11** gives the impression of a twisted triangular prism with sides of 8.8336(12) Å (as defined by the distances between platinum atoms), a side view reveals it to have more of a bowl shape, with access from two sides (see Fig. 10, left). The interior cavity is not empty, but rather filled with a water molecule (Fig. 11). Pt–Pt distances within the dinuclear edges are 2.9544(14) Å, and distances between centroids of opposite uracil rings are ca. 7.74 Å. Additional structural details are given in the Supporting Information.

2.9. Interrelationship between complexes described: A minimal formation scheme

In this paper we report on eight metal complexes containing the (twofold) deprotonated ligand **1** and the monodeprotonated ligand

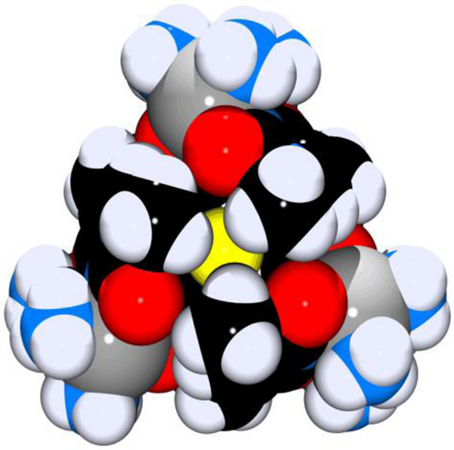

Fig. 11. Space filling representation of cation **11** with the inserted water molecule (yellow). (For interpretation of the references to color in this figure legend, the reader is referred to the web version of this article.)

2, respectively. In all cases reactions with *cis*-a_2M^{II} (M = Pt or Pd) in water lead to coordination of uracil-N3 sites, which become deprotonated. Despite relatively high pK_a values of the uracil moieties in **1** and **2**, metal coordination does not require high pH, as the *cis*-$[a_2M(H_2O)_2]^{2+}$ diaqua species occur as mixed hydroxo, aqua species at neutral or weakly acidic pH, and are thus capable of deprotonating the uracil rings with their hydroxo groups.

Ignoring differences in the nature of the metal M (Pt or Pd), the nature of the a_2 ligands (2,2′-bpy; bipzp; $(NH_3)_2$), and also in the two bis(uracil) ligands L (**1** and **2**), the similarities in structural features of the complexes characterized allow for a combined view on the products formed and permit a minimal reaction scheme for their formation to be put together. On the top of Scheme 6 simple complexes are drawn which, although not isolated, can be considered logical primary products to be formed between *cis*-a_2M^{II} and L, subject to reaction conditions (ratio of reactants, concentration, ...) and differences in kinetics (Pd^{II} reacting much faster than Pt^{II}). These primary products are expected to be of ML_2 (**I**), ML (**II**), and M_2L (**III**) stoichiometries. It is assumed that the first metal coordination takes place at N3 sites of the uracil entities, with the possible exception of Pt_2L, if favorable stacking interactions of the a_2 co-ligands (e.g., 2,2′-bpy) might favor the second M to bind to an exocyclic oxygen, most likely O4 (**IIIb**) rather than N3 at the other side of the ligand (**IIIa**). Starting out from these three (four) species, the formation of any of the various types of complexes reported here, can be rationalized in straightforward ways (Scheme 6, middle part). These are (i) the metallacycle **3** of M_2L_2 stoichiometry, (ii) the dimer **7** of likewise M_2L_2 stoichiometry, (iii) the tetranuclear complexes **5**, **6**, and **8** of M_4L_2 stoichiometries, (iv) the tetranuclear complex **9** of likewise M_4L_2 stoichiometry, and (v) the hexanuclear complex **11** of M_6L_3 stoichiometry. Complex **10** needs not to be discussed in this context, and we shall return to **4** as a model for additional possibilities of complex composition (see below). Possible rearrangement (isomerization) reactions between individual types of compounds shall not be further discussed, although they should not be excluded, in particular in the case of M = Pd, but even with M = Pt [31]. The possibility, that **9** could be the result of a minor rearrangement ("slippage") within **8** has been briefly mentioned. Alternatively, **9** could form in a stepwise reaction of ML_2 (**I**) upon successive coordination of three more metal entities M.

Complex **4** deserves some more comments (see also Scheme 6, bottom). In it, Ag^+ ions adopt unusual square-planar coordination geometries, involving O2 and O4 sites in their binding sites to uracilate anions. Instead of forming a coordination polymer, as realized in **4**, square-planar *cis*-a_2M^{II} entities could bind in the very same fashion to **3**, thereby producing yet another isomer of M_4L_2 stoichiometry, different from the linkage pattern realized in **5**, **6**, or **8** on one hand, and in **9** on the other. In fact, **9** with its mixed O2,O4

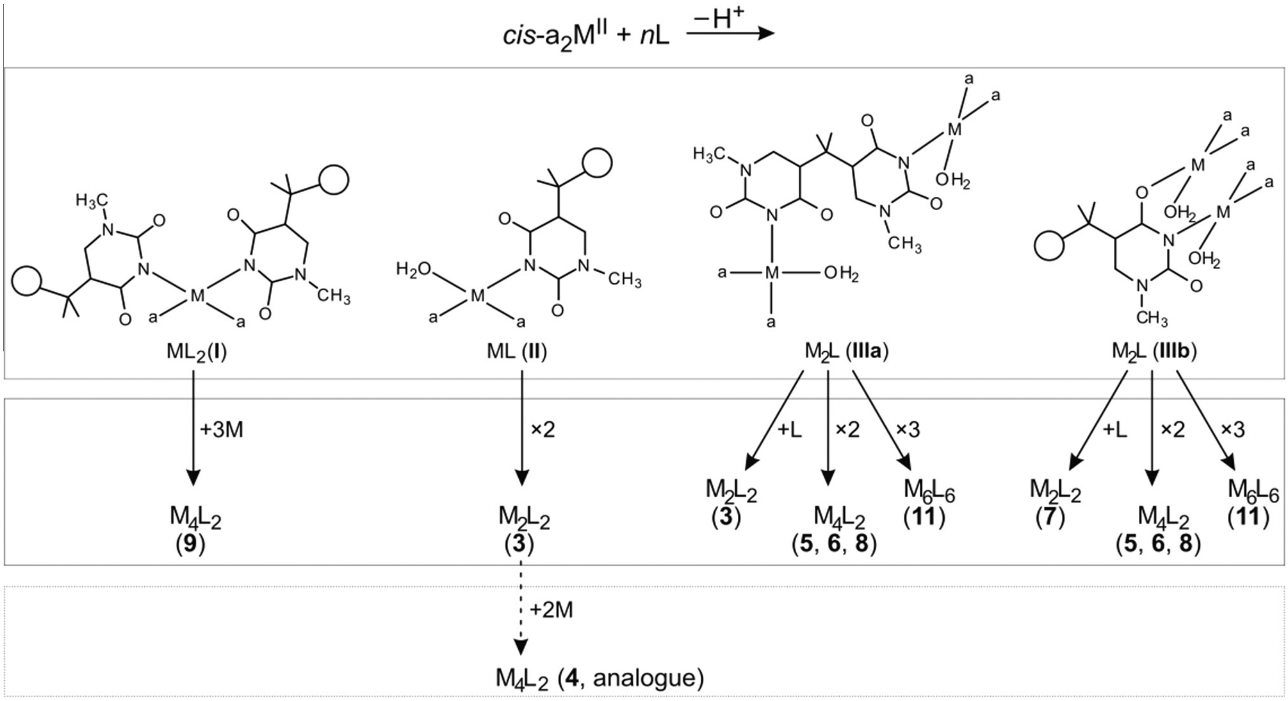

Scheme 6. Reaction products feasible and/or formed between *cis*-a_2M^{II} (M = Pt or Pd) and bis(1-methyluracil-5-yl)methane **1** (or related ligand **2**): Postulated initial products **I–III** (top), isolated species **3**, **5–9**, **11** (middle), and analogues derived on the basis of structure **4** (bottom). Additional possible isomers derived from ligand **1** in its cisoid conformation are not shown.

coordination sphere of one of the four Pt ions, can be considered an intermediate between the structures seen in **5**, **6**, **8** (with all-*ht* binding modes through N3 and O4) and the putative M_4L_2 analogue of **4** with mixed O2,O4 binding of two of the four metals. It is obvious, that with a larger excess of M, even products of M_5L_2 as well as M_6L_2 stoichiometries are feasible.

With the exception of **7**, all structurally characterized complexes have the bridging ligands **1**′ in transoid orientations. As briefly pointed out above (Section 2.3.) there is no compelling reason why the bis(1-methyluracil-5-yl)methane ligand in its deprotonated form (**1**′) should not be able to also adopt a cisoid arrangement and to form *cone* calixarene structures. If realized, yet additional linkage isomers of M_4L_2 stoichiometry would be possible, and in addition species of composition M_3L_2, M_5L_2, and M_6L_2. In the latter case, all eight exocyclic oxygen atoms of the four uracil rings would be occupied by metal ions, and in addition all four N3 sites.

3. Summary

In this manuscript we describe a series of metal complexes derived from *cis*-a_2M^{II} and bis(1-metyluracil-5-yl)methane ligands. With a single exception (complex **7**) all compounds are metallacycles, hence can be termed metallacalix[*n*]arenes. It strikes that all compounds except **3** contain stacked dimetal units. This feature is attributed to the pronounced basicity of the exocyclic oxygen atoms of uracil anions, as numerously demonstrated by us, and has some precedence in cyclic complexes of uracil and cytosine [3,5] as well as larger imidato ligands [32] or the cyanurato ligand with its three imide functionalities [33]. The complexity of the here discussed metallacalix[4]arenes is, among others, evident from the fact that species of M_4L_2 stoichiometry, for example, can conceivably exist in numerous isomeric variants, and that all species having *head–tail* disposed dimetal entities are inherently chiral. Structurally related cages (e.g., triangle [34], square [35], octahedron [36]) have also been synthesized by applying dimetal units with metal–metal bonds and tetradentate bridging ligands such as amidinates, oxalate, and dicarboxylates, but in these complexes the dimetal units do not represent stereogenic elements. In related work we have uncovered that metallacalix[4]arenes derived from the parent nucleobases uracil and cytosine can occur in a large number of isomeric forms [35], and have proposed that this feature may be one reason to account for the difficulty in fully characterizing a class of potent antitumor agents called “platinum pyrimidine blues” [37]. It appears that the here described bis(1-methyluracil-5-yl)methane ligand is similar as far as the complexity in terms of metal coordination by *cis*-a_2Pt^{II} is concerned.

4. Experimental

4.1. Starting materials and preparations

2,2′-bipyridine (2,2′-bpy), uracil, paraformaldehyde, benzaldehyde, HCl, K_2PtCl_4, K_2PdCl_4, $PdCl_2$, and $AgNO_3$ were of commercial origin and used as received without further purification. 1-Methyluracil [38], bis(pyrazol-1-yl)propane [39] bis(1-methyluracil-5-yl)methane monohydrate (**1**) [15] $PtCl_2$(2,2′-bpy) [40], and $PdCl_2$(2,2′-bpy) [41] were prepared as described in the literature.

4.2. Preparation of $PdCl_2$(bipzp)

This compound was prepared in a slightly modified version of that reported in Ref. [20]. $PdCl_2$ (285 mg, 1.60 mmol) was dissolved in refluxing acetonitrile (15 mL) and then cooled to room temperature. The solution was evaporated to dryness and the solid obtained was dissolved in 40 mL dichloromethane. The bis(pyrazol-1-yl)propane (282 mg, 1.60 mmol) was added and the resulting solution was stirred at room temperature for 12 h. The yellow solid was filtered off, washed with CH_2Cl_2 and dried at 40 °C. Yield: 500 mg (88%). *Anal.* Calc. for $C_9H_{12}N_4Cl_2Pd$: C, 30.6; H, 3.4; N, 15.9. Found: C, 30.4; H, 3.5; N, 16.8%. ^1H NMR ($CDCl_3$, 200 MHz, δ/ppm): 8.32 (H3, d, $^3J = 3.0$ Hz), 7.74 (H5, d, $^3J = 3.0$ Hz), 6.46 (H4, t, $^3J = 3.0$ Hz), 2.78 (CH_3, s).

4.3. Second polymorph of bis(1-methyluracil-5-yl)methane monohydrate (***1a***)

$AgNO_3$ (85 mg, 0.5 mmol) was added to a solution of **1** (52.8 mg, 0.2 mmol) in a 1:1-mixture of MeOH and water (2 mL), the mixture stirred for 2 h, and then left in a refrigerator at 4 °C for crystallization. Two days later, colorless crystals of **1a** were collected (30 mg, 57%). X-ray crystallography showed the crystals not to be a Ag complex of **1** but rather to be a second polymorph of the previously studied **1** [15].

4.4. Bis(1-methyluracil-5-yl)methyl-benzene (2)

This compound was synthesized in 90% yield according to a slightly modified version from that reported in the literature [15,17]. Specifically, 1-methyluracil was reacted with benzaldehyde in conc. HCl. ^1H NMR (DMSO-d_6, 298 K, δ, ppm): 11.32 (2H, s, N3–H), 7.03 (2H, s, C6–H), 5.09 (1H, s, C*H*Ph), 3.19 (6H, s, CH_3), 7.17 (2H, d, Ph), 7.24 (1H, dd, Ph), 7.32 (2H, dd, Ph).

4.5. [Pd(bipzp)(1′)]$_2$. in [Pd(bipzp)(1′)]$_2$·13H_2O (3)

A mixture of $PdCl_2$(bipzp) (353 mg, 1 mmol) and $AgNO_3$ (340 mg, 2 mmol) was stirred in water (50 mL) at 60 °C for 2.5 h in dark. The suspension obtained was cooled to 0 °C and the precipitated AgCl was subsequently removed by filtration. To the filtrate thus obtained, **1** (264 mg, 1 mmol) was added and pH of the solution adjusted to *ca* 9.0 by addition of aqueous 1 M NaOH solution. The reaction mixture was stirred overnight at 60 °C. The resulting solution was concentrated to 5 mL, centrifuged and left in a beaker at 4 °C. Prism shaped, light yellow crystals were obtained after two days (150.6 mg, 12%). *Anal.* Calc. for $C_{40}H_{62}N_{16}O_{17}Pd_2$ (9-hydrate): C, 38.4; H, 5.0; N, 17.9. Found: C, 38.4; H, 5.1; N, 18.0%. ^1H NMR (D_2O, pD 5.8, 298 K, δ, ppm): 8.120 (4H, d, H3′, $^3J_{H-H} = 2.5$ Hz), 7.632 (4H, s, H5′), 7.416 (4H, s, H6), 6.451 (4H, s, H4′), 3.356 (12H, s, CH_3), 3.076 (4H, s, CH_2), and 2.991 (12H, s, CH_3').

4.6. [{Pd(bipzp)(1′-N3)}$_2$(Ag–O2,O4)]$_n$ in [{Pd(bipzp)(1′-N3)}$_2$(Ag–O2,O4)]$_n$·15H_2O (**4**)

To an aqueous solution (3 mL) of **3** (65 mg, 0.05 mmol), 0.5 mL aqueous solution of $AgNO_3$ (42.5 mg, 0.25 mmol) was added with stirring. The formation of a colorless precipitate was observed. The reaction mixture was cooled in an ice bath for 2 h and the precipitate formed in due course was subsequently collected by filtration. Recrystallization from water (4 mL) yielded colorless single crystals (10.6 mg crystals, 10%). *Anal.* Calc. for $C_{40}H_{64}N_{17}O_{21}Pd_2Ag$ (5-hydrate): C, 35.6; H, 4.0; N, 17.6. Found: C, 35.5; H, 3.9; N, 17.6%. The ^1H NMR spectrum of **4** in D_2O is virtually identical with that of compound **3**, as can be expected.

4.7. ht,ht-{[Pd(2,2′-bpy)]$_2$(1′)}$_2$(H_3O)(NO_3)$_5$·8H_2O (**5**)

Pd(2,2′-bpy)Cl_2 (67 mg, 0.2 mmol) was stirred with $AgNO_3$ (68 mg, 0.4 mmol) in water (10 mL) with light excluded at 40 °C for 12 h. The suspension obtained was cooled to 0 °C in ice bath for 30 min. Then AgCl was removed from the solution by filtration.

Please cite this article in press as: A. Khutia et al., Inorg. Chim. Acta (2014), http://dx.doi.org/10.1016/j.ica.2014.01.020

1 (52.8 mg, 0.2 mmol) was added to the clear filtrate and pH was measured and found to be 2.0. Then the mixture was stirred at 40 °C for 2 h. The resulting light yellow solution was concentrated to a volume of 5 mL at 40 °C on a rotary evaporator. Yellow cubes were obtained after one day. The yield was 85 mg (60%). ^{1}H NMR (D_2O, pD 2.0, 298 K, δ, ppm): **1′**, 3.69 (12 H, s, CH_3), 3.60 (4H, s, CH_2), 7.93 (4H, s, H6); 2,2′-bpy, 7.23 (4H, dd, H5, $^3J_{H-H} = 6.0$ Hz, $^4J_{H-H} = 3.0$ Hz), 7.60 (4H, t, H5′, $^3J_{H-H} = 7.2$ Hz), 7.79 (4H, dd, H6, $^3J_{H-H} = 6.0$ Hz), 7.94–8.18 (20H, m, H3,H3′,H4,H4′,H6′).

4.8. *Second poymorph of ht,ht-{[Pt(2,2′-bpy)]$_2$(1′)}$_2$(NO$_3$)$_4$·12H$_2$O (**6**)*

This compound was prepared in analogy to the earlier reported one (8-hydrate) [15], except that the Pt:**1**-ratio had been altered, from 1:1 originally to 2:1 in the present case. X-ray crystallography of a suitable crystal proved it to be a second polymorph of the previously described compound.

4.9. *h,t-{[(2,2′-bpy)Pt]$_2$[1-MeU-N3,O4-CH(Ph)-1-MeUH]$_2$}$^{2+}$ (**7**)*

An aqueous suspension (30 mL) of $PtCl_2$(2,2′-bpy) (84.4 mg, 0.2 mmol) and $AgNO_3$ (68 mg, 0.4 mmol) was stirred for 24 h at 60 °C. The solution was cooled in ice for 1 h and the resultant AgCl precipitate was filtered off. **2** (68 mg, 0.2 mmol) was added and the solution was stirred for 3 days at 65 °C. The resulting solution was concentrated to a volume of 6 mL in a rotary evaporator, centrifuged, and filtered. The clear filtrate was kept in an open beaker at room temperature. After 4 d, 167 mg of dark red crystals were harvested. The compound was not obtained in analytically pure form, but a preliminary X-ray crystal structure of a crystal confirmed its dinuclear *head–tail* structure (see Ref. [1] and Supporting Information).

4.10. *ht,ht-{[cis-Pt(NH$_3$)$_2$]$_2$(1′)}$_2$(NO$_3$)$_4$·11H$_2$O (**8**)*

An aqueous suspension (20 mL) of *cis*-[$Pt(NH_3)_2Cl_2$] (120 mg, 0.4 mmol) and $AgNO_3$ (136 mg, 0.8 mmol) was stirred at 60 °C for 12 h. The solution was cooled in ice and the AgCl precipitate was filtered off. **1** (52.8 mg, 0.2 mmol) was added to the solution and the mixture was then stirred at 40 °C. The pH of the solution was repeatedly adjusted to 5 using 0.1 M NaOH solution. After one week the solution was concentrated to a volume of 3 mL, filtered and kept at 4 °C. After 4 days, colorless crystals were obtained. The yield was 131.7 mg (78%). *Anal.* Calc. for $C_{22}H_{44}N_{20}O_{20}Pt_4$: C, 15.7, H, 2.6, N, 16.6. Found: C, 15.4, H, 2.9, N, 16.3%. ^{1}H NMR (D_2O, pD 2.0, 298 K, δ, ppm): 3.08 (4H, s, CH_2), 3.54 (12H, s, CH_3), 7.45 (4H, s, H6). According to ^{1}H NMR spectroscopy, the compound isolated this way consisted exclusively of **8**, whereas slight modifications of the synthetic procedure yielded in addition other products (see below).

4.11. *hh,ht-{[cis-Pt(NH$_3$)$_2$(1′)}$_2$(NO$_3$)$_4$·9.5H$_2$O (**9**) and 2[ht,ht-{[cis-Pt(NH$_3$)$_2$]$_2$(1′)}$_2$]·[hh,ht-{[cis-Pt(NH$_3$)$_2$]$_2$(1′)}$_2$](NO$_3$)$_{12}$·16H$_2$O (**10**)*

(a) An aqueous suspension (3 mL) of *cis*-$Pt(NH_3)_2Cl_2$ (120 mg, 0.4 mmol) and $AgNO_3$ (136 mg, 0.8 mmol) was stirred at 60 °C for 12 h. The solution was then cooled in ice and the AgCl precipitate was filtered off. **1** (52.8 mg, 0.2 mmol) was added to the solution and the pH of the solution was adjusted to 5 using 0.1 M NaOH solution (one time). The mixture was then stirred at 40 °C for one week. The solution was subsequently centrifuged from some unidentified precipitate and the filtrate was kept at 4 °C. It adopted a light blue color within two days. Colorless crystals were harvested after five days. One crystal was picked from solution for X-ray analysis and proved to be **9**.

(b) The same reaction was carried out under identical conditions as procedure (a), yet at higher dilution (20 mL). Here also colorless crystals were obtained after six days, and one crystal was measured by X-ray crystallography, which proved to be complex **10**, a 2:1 adduct of **8** and **9**.

The ^{1}H NMR spectra of the isolated solids suggest that procedures (a) and (b) lead to qualitatively similar mixtures of **8** and **9**, with **9** representing the major species. The crystals of complex **8** and complex **9** have practically identical shapes and cannot be separated under a microscope.

4.12. *ht,ht,ht-{[cis-Pt(ND$_3$)$_2$(1′)]$_3$(NO$_3$)$_6$·9D$_2$O (**11**)*

cis-$Pt(NH_3)_2Cl_2$ (60 mg, 0.2 mmol) was mixed with $AgNO_3$ (68 mg, 0.4 mmol,) in D_2O (2 mL) with light excluded and stirred at 80 °C for 2 h. The suspension obtained was cooled to 0 °C in an ice bath for 30 min. Then AgCl was removed from the solution by centrifugation. **1** (26.4 mg, 0.1 mmol) was added to the filtrate and the pD was adjusted to 5.0 by adding NaOD. Then the mixture was warmed at 40 °C for 7 d. After centrifugation of some precipitate, which was not further characterized, the resulting solution was kept in a refrigerator at 4 °C for several days. During the time the color of the solution turned dark blue. Needle shaped, light green crystals were obtained after 1 week. The isolated yield was ca. 5 mg, 6%. A crystal with an appearance different from that of either **8** or **9** was picked for X-ray analysis and showed it to be compound **11**. The ^{1}H NMR spectrum of the isolated material (D_2O, pD 5.2) was practically identical with that of complex **8**, however, suggesting that **11** was a very minor component only or that it had formed from **8** during the final crystallization step. Monitoring the reaction on an NMR scale likewise did not reveal any strong indication for the existence of another species besides **8** or **9** in solution. We rule out that **8** and **11** could have identical ^{1}H NMR spectra, despite identical N3, O4 binding patterns.

4.13. *Instrumentation*

^{1}H NMR spectra were recorded on Bruker AC 300 and Bruker DRX 400 NMR instruments with 3-(trimethylsilyl)propanesulfonate (TSP, $\delta = 0$ ppm) as internal reference in D_2O and the solvent residual peak ($\delta = 2.50$ ppm) as reference for DMSO-d_6. Elemental (C, H, N) analysis data were obtained on a Leco CHNS-932 instrument. In the large majority of cases elemental analysis data gave values which agreed with significantly lower water contents than established by X-ray analysis

4.14. *Determination of pK$_a$ values*

The pK_a values of **2** were determined by pD-dependent ^{1}H NMR spectroscopy. The changes in chemical shift of the C6–*H* and N1–CH_3 (no change for C*H*(Ph) proton) protons were recorded at the different pD stages. pD values of NMR samples were measured by use of a glass electrode and addition of 0.4 units to the uncorrected pH meter reading (pH*). pD values were varied by addition of NaOD and DNO_3 to the respective samples. The graphs (chemical shift versus pD) were evaluated with a nonlinear least-squares fit according to the Newton–Gauss method [42] The obtained acidity constants (for D_2O) were transformed to values valid for H_2O [43].

4.15. *X-ray crystallography*

X-ray crystal data collections for **1a**, **3**, **4**, **5**, **6**, **8**, **9**, and **11** were recorded at 150 K on an Xcalibur Sapphire3 diffractometer equipped with an area detector and graphite monochromated Mo Kα radiation (0.71073 Å). Data reduction was performed using the CRYSALISPRO software package [44]. The structures were solved by direct methods and refined by full-matrix least-squares methods based on F^2 using the SHELXL-97 programs [45]. All non-hydrogen atoms were refined anisotropically with thermal and distance restraints applied when necessary. Hydrogen atoms were positioned geometrically and refined with isotropic displacement parameters according to the riding model. All calculations were carried out with the SHELXL-97 and WINGX programs [45,46].

*4.15.1. Crystal data for **1a***

$[C_{11}H_{14}N_4O_5]$, triclinic, $P2_1/c$, $a = 8.2374(3)$ Å, $b = 8.7690(4)$ Å, $c = 17.0166(7)$ Å, $\beta = 95.547(4)°$, $Z = 4$, $M_r = 282.26$ g mol^{-1}, $V = 1223.42(9)$ Å^3, $D_{calc.} = 1.532$ g cm^{-3}, λ(Mo Kα) = 0.71073 Å, $T = 150$ K, $\mu = 0.123$ mm^{-1}, 23787 reflections collected, 3061 observed ($R_{int} = 0.0511$), $R_1(F_o) = 0.0381$ [$I > 2\sigma(I)$], $wR_2(F_o^2) = 0.0742$ (all data), Goodness-of-fit (GOF) = 0.990. CCDC 974350.

*4.15.2. Crystal data for **3***

$[C_{40}H_{70}N_{16}O_{21}Pd_2]$, triclinic, $P\bar{1}$, $a = 12.3877(5)$ Å, $b = 14.7605(5)$ Å, $c = 15.7897(6)$ Å, $\alpha = 86.764(3)°$, $\beta = 75.852(3)°$, $\gamma = 80.895(3)°$, $Z = 2$, $M_r = 1323.92$ g mol^{-1}, $V = 2763.80(18)$ Å^3, $D_{calc.} = 1.591$ g cm^{-3}, λ(Mo Kα) = 0.71073 Å, $T = 150$ K, $\mu = 0.740$ mm^{-1}, 23780 reflections collected, 12452 observed ($R_{int} = 0.0332$), $R_1(F_o) = 0.0315$ [$I > 2\sigma(I)$], $wR_2(F_o^2) = 0.0561$ (all data), Goodness-of-fit (GOF) = 0.839. CCDC 974351.

*4.15.3. Crystal data for **4***

$[C_{40}H_{74}AgN_{17}O_{26}Pd_2]$, triclinic, $P\bar{1}$, $a = 13.4345(10)$ Å, $b = 15.2333(13)$ Å, $c = 17.3649(15)$ Å, $\alpha = 71.703(8)°$, $\beta = 67.541(8)°$, $\gamma = 77.475(7)°$, $Z = 2$, $M_r = 1529.83$ g mol^{-1}, $V = 3099.1(4)$ Å^3, $D_{calc.} = 1.639$ g cm^{-3}, λ(Mo Kα) = 0.71073 Å, $T = 150$ K, $\mu = 0.979$ mm^{-1}, 25456 reflections collected, 13735 observed ($R_{int} = 0.0772$), $R_1(F_o) = 0.1092$ [$I > 2\sigma(I)$], $wR_2(F_o^2) = 0.3038$ (all data), Goodness-of-fit (GOF) = 1.054. CCDC 974352.

*4.15.4. Crystal data for **5***

$[C_{62}H_{71}N_{21}O_{32}Pd_4]$, monoclinic, $P2_1/c$, $a = 10.4660(9)$ Å, $b = 47.844(3)$ Å, $c = 15.4389(13)$ Å, $\beta = 104.141(8)°$, $Z = 4$, $M_r = 2048.00$ g mol^{-1}, $V = 7496.5(10)$ Å^3, $D_{calc.} = 1.815$ g cm^{-3}, λ(Mo Kα) = 0.71073 Å, $T = 150$ K, $\mu = 1.048$ mm^{-1}, 38845 reflections collected, 16431 observed ($R_{int} = 0.1765$), $R_1(F_o) = 0.2173$ [$I > 2\sigma(I)$], $wR_2(F_o^2) = 0.4871$ (all data), Goodness-of-fit (GOF) = 1.005. CCDC 974353.

*4.15.5. Crystal data for **6***

$[C_{62}H_{76}N_{20}O_{32}Pt_4]$, triclinic, $P\bar{1}$, $a = 14.4817(5)$ Å, $b = 22.4096(9)$ Å, $c = 24.7764(9)$ Å, $\alpha = 99.061(3)°$, $\beta = 94.446(3)°$, $\gamma = 101.702(3)°$, $Z = 4$, $M_r = 2393.79$ g mol^{-1}, $V = 7725.3(5)$ Å^3, $D_{calc.} = 2.058$ g cm^{-3}, λ(Mo Kα) = 0.71073 Å, $T = 150$ K, $\mu = 7.321$ mm^{-1}, 63581 reflections collected, 34457 observed ($R_{int} = 0.0777$), $R_1(F_o) = 0.0927$ [$I > 2\sigma(I)$], $wR_2(F_o^2) = 0.2338$ (all data), Goodness-of-fit (GOF) = 1.001. CCDC 974354.

*4.15.6. Crystal data for **7***

$[C_{54}H_{98}N_{14}O_{40}Pt_2]$, monoclinic, $C2/c$, $a = 23.5996(7)$ Å, $b = 26.8002(10)$ Å, $c = 14.5305(5)$ Å, $\beta = 91.934(3)°$, $Z = 4$, $M_r = 1973.64$ g mol^{-1}, $V = 9184.9(5)$ Å^3, $D_{calc.} = 1.427$ g cm^{-3}, λ(Mo Kα) = 0.71073 Å, $T = 150$ K, $\mu = 3.129$ mm^{-1}, 29426 reflections collected, 10627 observed ($R_{int} = 0.0385$), $R_1(F_o) = 0.0337$ [$I > 2\sigma(I)$], $wR_2(F_o^2) = 0.0900$ (all data), Goodness-of-fit (GOF) = 0.988. CCDC 974355.

*4.15.7. Crystal data for **8***

$[C_{22}H_{55}N_{20}O_{31}Pt4]$, monoclinic, $P2_1/n$, $a = 10.9959(5)$ Å, $b = 30.3044(16)$ Å, $c = 17.0166(7)$ Å, $\beta = 104.296(5)°$, $Z = 4$, $M_r = 1887.31$ g mol^{-1}, $V = 5494.8(4)$ Å^3, $D_{calc.} = 2.281$ g cm^{-3}, λ(Mo Kα) = 0.71073 Å, $T = 150$ K, $\mu = 10.257$ mm^{-1}, 27200 reflections collected, 12005 observed ($R_{int} = 0.0812$), $R_1(F_o) = 0.0778$ [$I > 2\sigma(I)$], $wR_2(F_o^2) = 0.2019$ (all data), Goodness-of-fit (GOF) = 0.970. CCDC 974347.

*4.15.8. Crystal data for **9***

$[C_{44}H_{164}N_{40}O_{59}Pt_8]$, monoclinic, $P2_1/c$, $a = 20.1556(16)$ Å, $b = 29.455(2)$ Å, $c = 21.743(3)$ Å, $\beta = 121.358(8)°$, $Z = 4$, $M_r = 3758.87$ g mol^{-1}, $V = 11022.9(19)$ Å^3, $D_{calc.} = 2.265$ g cm^{-3}, λ(Mo Kα) = 0.71073 Å, $T = 150$ K, $\mu = 10.223$ mm^{-1}, 53944 reflections collected, 25506 observed ($R_{int} = 0.0871$), $R_1(F_o) = 0.0598$ [$I > 2\sigma(I)$], $wR_2(F_o^2) = 0.1251$ (all data), Goodness-of-fit (GOF) = 0.973. CCDC 974348.

*4.15.9. Crystal data for **11***

$[C_{33}H_{81}N_{30}O_{40}Pt_6]$, trigonal, $P–31c$, $a = 16.9534(9)$ Å, $c = 18.0896(9)$ Å, $Z = 2$, $M_r = 2708.82$ g mol^{-1}, $V = 4502.7(4)$ Å^3, $D_{calc.} = 1.998$ g cm^{-3}, λ(Mo Kα) = 0.71073 Å, $T = 150$ K, $\mu = 9.377$ mm^{-1}, 41046 reflections collected, 3831 observed ($R_{int} = 0.0540$), $R_1(F_o) = 0.0785$ [$I > 2\sigma(I)$], $wR_2(F_o^2) = 0.2271$ (all data), Goodness-of-fit (GOF) = 1.076. CCDC 974349.

Acknowledgements

This work was supported by Deutsche Forschungsgemeinschaft (DFG), the “International Max Planck Research School in Chemical Biology” in Dortmund (for a fellowship to A.K.) and DAAD (for a “Forschungsaufenthalt” award to N.D.). P.J.S.M. thanks funding from the Spanish Ministerio de Economía y Competitividad (“Ramón y Cajal” program and CTQ2011-27593). We thank Ms Stefanie Seidel for experimental assistance.

Appendix A. Supplementary material

NMR spectra and pH dependence of compound **2**. CCDC 974347–974354 contain the supplementary crystallographic data (**1a**, **3**, **4**, **5**, **6**, **8**, **9**, and **11**). These data can be obtained free of charge from The Cambridge Crystallographic Data Centre via www.ccdc.cam.ac.uk/data_request/cif. Supplementary data associated with this article can be found, in the online version, at http://dx.doi.org/10.1016/j.ica.2014.01.020.

References

[1] C.D. Gutsche, Calixarenes, The Royal Society of Chemistry, Cambridge, 1989.
[2] (a) M.-X. Wang, Chem. Commun. (2008) 4541. and refs. cited;
(b) B. König, M.H. Fonseca, Eur. J. Inorg. Chem. (2000) 2303.
[3] (a) H. Rauter, E.C. Hillgeris, B. Lippert, J. Chem. Soc., Chem. Commun. (1992) 1385;
(b) H. Rauter, E.C. Hillgeris, A. Erxleben, B. Lippert, J. Am. Chem. Soc. 116 (1994) 616.
[4] (a) J.A.R. Navarro, M.B.L. Janik, E. Freisinger, B. Lippert, Inorg. Chem. 38 (1999) 426;
(b) J.A.R. Navarro, J.M. Salas, Chem. Commun. (2000) 235;
(c) J.A.R. Navarro, E. Freisinger, B. Lippert, Inorg. Chem. 39 (2000) 2301;
(d) J.A.R. Navarro, B. Lippert, B. Coord. Chem. Rev. 222 (2001) 219;
(e) M.A. Galindo, J.M. Salas, M.A. Romero, M. Quirós, N. Masciocchi, S. Galli, A. Sironi, B. Lippert, J. Solid State Chem. 178 (2005) 2436;
(f) E. Barea, J.A.R. Navarro, J.M. Salas, M. Quirós, M. Willermann, B. Lippert, Chem. Eur. J. 13 (2007) 6019.
[5] (a) E.G. Bardají, E. Freisinger, B. Costisella, C.A. Schalley, W. Brüning, M. Sabat, B. Lippert, Chem. Eur. J. 13 (2007) 6019;
(b) A. Khutia, P.J. Sanz, Inorg. Chem. 49 (2010) 7635;
(c) A. Khutia, P.J. Sanz, Chem. Eur. J. 17 (2011) 4195;
(d) A. Khutia, P.J. Sanz, Chem. Eur. J. 17 (2011) 4205.
[6] (a) S. Ibáñez, F.M. Albertí, P.J. Sanz, Chem. Eur. J. 17 (2011) 9283;
(b) A. Galstyan, W.-Z. Shen, E. Freisinger, H. Alkam, W. Hiller, P.J. Sanz Miguel, M. Schürmann, B. Lippert, Chem. Eur. J. 17 (2011) 10771. and refs. cited;
(c) C. Price, M.A. Shipman, N.H. Rees, M.R.J. Elsegood, A.J. Edwards, W. Clegg, A. Houlton, Chem. Eur. J. 7 (2001) 1194.
[7] Reviews: (a) S. Leininger, B. Olenyuk, P.J. Stang, Chem. Rev. 100 (2000) 853;
(b) B.J. Holliday, C.A. Mirkin, Angew. Chem., Int. Ed. 40 (2001) 2022;

Please cite this article in press as: A. Khutia et al., Inorg. Chim. Acta (2014), http://dx.doi.org/10.1016/j.ica.2014.01.020

(c) M. Fujita, M. Tominaga, A. Hori, B. Therrien, Acc. Chem. Res. 38 (2005) 369;
(d) A. Kaiser, P. Bäuerle, Top. Curr. Chem. 249 (2005) 127;
(e) G. Mezei, C.M. Zaleski, V.L. Pecoraro, Chem. Rev. 107 (2007) 4933;
(f) E. Zangrando, M. Casanova, E. Alessio, Chem. Rev. 108 (2008) 4979;
(g) A. Kumar, S.S. Sun, A.J. Lees, Coord. Chem. Rev. 252 (2008) 922;
(h) B. Lippert, P.J. Sanz, Miguel, Chem. Soc. Rev. 40 (2011) 4475.

[8] Historical perspectives: (a) J. Harrowfield, Chem. Commun. 49 (2013) 1578;
(b) A. Casnati, Chem. Commun. 49 (2013) 6827.

[9] Selected examples for rim/bridge metal binding: (a) D. Buccella, G. Parkin, Chem. Commun. (2009) 289;
(b) D. Mendoza-Espinosa, T.A. Hanna, Inorg. Chem. 48 (2009) 7452;
(c) C. Redshaw, D. Homden, D.L. Hughes, J.A. Wright, M.R.J. Elsegood, Dalton Trans. (2009) 1231;
(d) U. Darost, O. Sénèque, Y. Li, G. Bertho, J. Marrot, M.-N. Rager, O. Reinaud, I. Jabin, Chem. Eur. J. 13 (2007) 2078;
(e) T. Kajiwara, K. Katagiri, M. Hasegawa, A. Ishii, M. Ferbinteanu, S. Takaishi, T. Ito, M. Yamashita, N. Iki, Inorg. Chem. 45 (2006) 4880;
(f) N. Kotzen, I. Goldberg, S. Lipstman, A. Vigalok, Inorg. Chem. 45 (2006) 5266;
(g) J. Zeller, U. Radius, Inorg. Chem. 45 (2006) 9487.

[10] Selected examples for metal binding to dangling groups: (a) A. Ovsyannikov, S. Ferlay, S.E. Solovieva, I.S. Antipin, A.I. Konovalov, N. Kyritsakas, M.W. Hosseini, Dalton Trans. 42 (2013) 9946;
(b) D.T. Schühle, J. Schatz, S. Laurent, L. Vander Elst, R.N. Muller, M.C.A. Stuart, J.A. Peters, Chem. Eur. J. 15 (2009) 3290;
(c) R. Cacciapaglia, A. Casnati, L. Mandolini, D.N. Reinhoudt, R. Salvio, A. Sartori, R. Ungaro, J. Am. Chem. Soc. 128 (2006) 12322;
(d) B.H. Brodsky, J. Du Bois, Chem. Commun. (2006) 4715;
(e) D.J. Eisler, R.J. Puddephatt, Inorg. Chem. 44 (2005) 4666;
(f) J. McGinley, V. McKee, J.M.D. Walsh, Inorg. Chim. Acta 375 (2011) 57.

[11] (a) M.A. Galindo, D. Olea, M.A. Romero, J. Gómez, P. Del Castillo, M.J. Hannon, A. Rodger, F. Zamora, J.A.R. Navarro, Chem. Eur. J. 13 (2007) 5075;
(b) M.A. Galindo, M. Angustias, Inorg. Chim. Acta 362 (2009) 1027.

[12] (a) M.A. Galindo, J.A.R. Navarro, M. Angustias Romero, M. Quirós, Dalton Trans. (2004) 1563;
(b) M.A. Galindo, A. Houlton, W. Clegg, R.W. Harrington, J. Dobado, F. Santoya-Gonzalez, F. Linares, M. Angustias, Chem. Commun. (2008) 3735.

[13] (a) H. Rauter, I. Mutikainen, M. Blomberg, C.J.L. Lock, P. Amo-Ochoa, E. Freisinger, L. Randaccio, E. Zangrando, E. Chiarparin, B. Lippert, Angew. Chem., Int. Ed. Engl. 36 (1997) 1296;
(b) J.A.R. Navarro, E. Freisinger, B. Lippert, Eur. J. Inorg. Chem. (2000) 147.

[14] (a) F. Guay, A.L. Beauchamp, J. Am. Chem. Soc. 101 (1979) 6260;
(b) K. Aoki, W. Saenger, Acta Crystallogr., Sect. C 40 (1984) 775;
(c) B. Lippert, Prog. Inorg. Chem. 37 (1989) 1. and refs. cited;
(d) W. Chen, K. Matsumoto, Eur. J. Inorg. Chem. (2002) 2664;
(e) W. Chen, F. Liu, D. Xu, K. Matsumoto, S. Kishi, M. Kato, Inorg. Chem. 45 (2006) 5552;
(f) W. Chen, F. Liu, K. Matsumoto, J. Autschbach, B. Le Guennic, T. Ziegler, M. Maliarik, J. Glaser, Inorg. Chem. 45 (2006) 4526;
(g) K. Uemura, M. Ebihara, Inorg. Chem. 52 (2013) 5535.

[15] N. Das, P.J. Sanz Miguel, A. Khutia, M. Lazar, B. Lippert, Dalton. Trans. (2009) 9120.

[16] S. Chakraborty, P.J. Sanz Miguel, F.M. Albertí, N. Das, J. Mol. Struct. 1015 (2012) 99.

[17] S. Kumar, V. Malik, N. Kaur, K. Kaur, Tetrahedron Lett. 47 (2006) 8483.

[18] K.L. Wierzchowski, E. Litonska, D. Shugar, J. Am. Chem. Soc. 87 (1965) 4621.

[19] P.A. Levene, L.W. Bass, H.S. Simms, J. Biol. Chem. 70 (1926) 229.

[20] G. Minghetti, M. Cinellu, A.L. Bandini, G. Banditelli, F. Demartin, M. Manassero, J. Organomet. Chem. 315 (1986) 387.

[21] M. Fujita, M. Aoyagi, K. Ogura, Inorg. Chim. Acta 246 (1996) 53.

[22] M. Schmitz, S. Leininger, J. Fan, A.M. Arif, P.J. Stang, Organometallics 18 (1999) 4817.

[23] F.M. Albertí, T. Mihály, B. Lippert, P.J. Sanz Miguel, CrystEngComm 14 (2012) 6178–6181. and refs. cited.

[24] H. Schöllhorn, U. Thewalt, B. Lippert, J. Chem. Soc., Chem. Commun. (1984) 769.

[25] A.G. Young, L.R. Hanton, Coord. Chem. Rev. 252 (2008) 1346.

[26] B. Lippert, D. Neugebauer, Inorg. Chem. 21 (1982) 451.

[27] (a) B. Lippert, H. Schöllhorn, U. Thewalt, Inorg. Chem. 26 (1987) 1736;
(b) F. Zamora, H. Witkowski, E. Freisinger, J. Müller, B. Thormann, A. Albinati, B. Lippert, J. Chem. Soc., Dalton Trans. (1999) 175.

[28] See, e.g.: (a) T. Yamaguchi, F. Yamazaki, T. Ito, J. Am. Chem. Soc. 123 (2001) 743;
(b) J. Forniés, S. Ibánez, E. Lalinde, A. Martín, M.T. Moreno, A.C. Tsipis, Dalton Trans. 41 (2012) 3439.

[29] W.-Z. Shen, G. Trötscher-Kaus, B. Lippert, Dalton Trans. (2009) 8203.

[30] See, e.g.: (a) P.K. Mascharak, I.D. Williams, S.J. Lippard, J. Am. Chem. Soc. 106 (1984) 6428;
(b) B. Lippert, Chimia 61 (2007) 732.

[31] (a) T.V. O'Halloran, S.J. Lippard, Inorg. Chem. 28 (1989) 1289;
(b) S. Iwatsuki, T. Itou, H. Ito, H. Mori, K. Uemura, Y. Yokomori, K. Ishihara, K. Matsumoto, Dalton Trans. (2006) 1497.

[32] H.M. Colquhoun, R.A. Fairman, P. Tootell, D.J. Williams, J. Chem. Soc., Dalton Trans. (1999) 2651.

[33] C.A. Murray, C.J. Cardin, B.W. Greenland, A. Swift, H.M. Colquhoun, Inorg. Chem. 52 (2013) 10424.

[34] F.A. Cotton, C. Lin, C.A. Murillo, Inorg. Chem. 40 (2001) 575.

[35] (a) B.E. Bursten, M.H. Chisholm, C.M. Hadad, J. Li, P.J. Wilson, Chem. Commun. (2001) 2382;
(b) J.F. Brickley, R.P. Bonar-Law, C. Femoni, E.J. MacLean, A. Steiner, S.J. Teat, J. Chem. Soc., Dalton Trans. (2000) 4025.

[36] F.A. Cotton, C. Lin, C.A. Murillo, Inorg. Chem. 40 (2001) 6413.

[37] J.P. Davidson, P.J. Faber, R.G. Fischer Jr., S. Mansy, H.J. Peresie, B. Rosenberg, L. VanCamp, Cancer Chemother. Rep. Part I 59 (1975) 287.

[38] W. Micklitz, B. Lippert, H. Schölhorn, U. Thewalt, J. Heterocycl. Chem. 26 (1989) 1499.

[39] S. Tsuji, D.C. Swenson, R.F. Jordan, Organometallics 18 (1999) 4758.

[40] G.T. Morgan, F.H. Burstall, J. Chem. Soc. (1934) 965.

[41] B.J. McCormick, E.N. Jaynes Jr., R. Kaplan, Inorg. Synth. 13 (1972) 216.

[42] R. Tribolet, H. Sigel, Eur. J. Biochem. 163 (1987) 353.

[43] R.B. Martin, Science 139 (1963) 1198.

[44] CRYSALISPRO, Oxford Diffraction, Poland, 2008.

[45] G.M. Sheldrick, SHELX-97, University of Göttingen, Göttingen, Germany, 1997.

[46] L.J. Farrugia, WINGX, University of Glasgow, Great Britain, 1998.

Please cite this article in press as: A. Khutia et al., Inorg. Chim. Acta (2014), http://dx.doi.org/10.1016/j.ica.2014.01.020